

# Islet Microenvironment, Modulated by Vascular Endothelial Growth Factor-A Signaling, Promotes $\beta$ Cell Regeneration

Marcela Brissova,<sup>1,6,\*</sup> Kristie Aamodt,<sup>2,6</sup> Priyanka Brahmachary,<sup>1,6</sup> Nripesh Prasad,<sup>3,4</sup> Ji-Young Hong,<sup>1</sup> Chunhua Dai,<sup>1</sup> Mahnaz Mellati,<sup>1</sup> Alena Shostak,<sup>1</sup> Greg Poffenberger,<sup>1</sup> Radhika Aramandla,<sup>1</sup> Shawn E. Levy,<sup>3</sup> and Alvin C. Powers<sup>1,2,5,\*</sup>

<sup>1</sup>Division of Diabetes, Endocrinology, and Metabolism, Department of Medicine

<sup>2</sup>Department of Molecular Physiology and Biophysics

Vanderbilt University Medical Center, Nashville, TN 37232, USA

<sup>3</sup>HudsonAlpha Institute for Biotechnology, Huntsville, AL 35806, USA

<sup>4</sup>Department of Biology, University of Alabama, Huntsville, Huntsville, AL 35899, USA

<sup>5</sup>VA Tennessee Valley Healthcare System, Nashville, TN 37212, USA

<sup>6</sup>These authors contributed equally to this work

\*Correspondence: [marcela.brissova@vanderbilt.edu](mailto:marcela.brissova@vanderbilt.edu) (M.B.), [al.powers@vanderbilt.edu](mailto:al.powers@vanderbilt.edu) (A.C.P.)

<http://dx.doi.org/10.1016/j.cmet.2014.02.001>

## SUMMARY

Pancreatic islet endocrine cell and endothelial cell (EC) interactions mediated by vascular endothelial growth factor-A (VEGF-A) signaling are important for islet differentiation and the formation of highly vascularized islets. To dissect how VEGF-A signaling modulates intra-islet vasculature, islet microenvironment, and  $\beta$  cell mass, we transiently increased VEGF-A production by  $\beta$  cells. VEGF-A induction dramatically increased the number of intra-islet ECs but led to  $\beta$  cell loss. After withdrawal of the VEGF-A stimulus,  $\beta$  cell mass, function, and islet structure normalized as a result of a robust, but transient, burst in proliferation of pre-existing  $\beta$  cells. Bone marrow-derived macrophages (M $\Phi$ s) recruited to the site of  $\beta$  cell injury were crucial for the  $\beta$  cell proliferation, which was independent of pancreatic location and circulating factors such as glucose. Identification of the signals responsible for the proliferation of adult, terminally differentiated  $\beta$  cells will improve strategies aimed at  $\beta$  cell regeneration and expansion.

## INTRODUCTION

Pancreatic islets are highly vascularized and contain a structurally and functionally unique capillary network where each  $\beta$  cell is in cellular proximity to ECs (Brissova et al., 2006; Nyman et al., 2008). ECs produce instructive signals necessary for early pancreatic endoderm specification and endocrine cell differentiation (Lammert et al., 2001; Yoshitomi and Zaret, 2004), but several recent studies proposed that requirements for blood vessel-derived signals may differ between early and later stages of pancreas development (Cai et al., 2012; Magenheim et al., 2011; Reinert et al., 2014; Sand et al., 2011). VEGF-A produced by islet endocrine cells is a principal regulator of islet vascular development and vascular homeostasis (Brissova et al., 2006;

Lammert et al., 2003). Inactivation of VEGF-A, either in endocrine progenitors or differentiated  $\beta$  cells, leads to a profound loss of intra-islet capillary density, vascular permeability, and islet function. Though it is clear that altering islet microvasculature affects insulin delivery into peripheral circulation, the role of intra-islet ECs and the VEGF-A signaling pathway in regulating adult  $\beta$  cell mass is not fully understood. Work by Lammert and colleagues suggests that continuous pancreas-wide overexpression of VEGF-A from early development to adulthood results in pancreatic hypervascularization,  $\beta$  cell mass expansion, and islet hyperplasia (Lammert et al., 2001). However, a more recent report by Agudo et al. reveals that VEGF-A-stimulated intra-islet EC expansion in adult islets is associated with reduced  $\beta$  cell mass (Agudo et al., 2012).

$\beta$  cells of the pancreatic islet have an extremely limited regenerative potential, so there are major efforts to foster  $\beta$  cell regeneration in type 1 and type 2 diabetes. Recent studies have identified several systemic factors and signaling pathways implicated in  $\beta$  cell replication during increased metabolic demand and following injury (Porat et al., 2011; Rieck and Kaestner, 2010), but the role of local islet molecular and cellular factors in  $\beta$  cell regeneration, and in particular human  $\beta$  cell regeneration, is unknown.

Increasing evidence suggests that local organ-specific vascular niches are determinant in organ repair and tumorigenesis where ECs produce tissue-specific paracrine growth factors, defined as angiocrine factors (Butler et al., 2010a). VEGF-A signaling through its obligatory VEGFR2 receptor plays a critical role in this process. In addition to this emerging role for the VEGF-A signaling pathway in organ regeneration via angiocrine signaling, local increases in VEGF-A production during tissue injury and tumorigenesis lead to homing of bone marrow-derived cells (BMCs), especially monocytes, which express the VEGFR1 receptor (Barleon et al., 1996). While these cells may enhance VEGF-induced neovascularization, they also actively participate in tissue repair.

To investigate how VEGF-A signaling modulates intra-islet vasculature, islet microenvironment, and  $\beta$  cell mass, we transiently increased  $\beta$  cell VEGF-A production in mature mouse islets ( $\beta$ VEGF-A model). This increased production of VEGF-A

in  $\beta$  cells dramatically increases intra-islet EC proliferation, but surprisingly leads to a rapid loss of  $\beta$  cells. Remarkably, 6 weeks after removing the VEGF-A stimulus, islet morphology, vascularization, mass, and function normalize due to replication of pre-existing  $\beta$  cells. Using an islet transplantation model with wild-type (WT) and  $\beta$ VEGF-A islets transplanted under contralateral kidney capsules with or without human islets, we demonstrate that this  $\beta$  cell replication is independent of the pancreatic site and circulating factors and is not limited to murine  $\beta$  cells. Our studies indicate that the local islet microenvironment modulated by VEGF-A signaling can play an integral role in  $\beta$  cell regeneration. This process depends on VEGF-A-mediated recruitment of M $\Phi$ s, which, either directly or cooperatively with quiescent intra-islet ECs, induce  $\beta$  cell proliferation.

## RESULTS

### Increased $\beta$ Cell VEGF-A Production Leads to Islet EC Expansion and $\beta$ Cell Loss Followed by $\beta$ Cell Regeneration after VEGF-A Normalizes

To dissect the role of the VEGF-A signaling pathway in regulating adult  $\beta$  cell mass, we used a mouse model of doxycycline (Dox)-inducible  $\beta$  cell-specific overexpression of human VEGF-A<sup>164</sup> ( $\beta$ VEGF-A) (Efrat et al., 1995; Ohno-Matsui et al., 2002). Islet VEGF-A production increased rapidly within 24 hr of Dox treatment (Figure S1A), and robust proliferation of intra-islet ECs was observed 72 hr after VEGF-A induction (Figure S1B). We found that a transient increase in  $\beta$  cell VEGF-A production for 1 week dramatically increased the number of intra-islet ECs and led to a substantial loss of  $\beta$  cells (Figures 1A and 1B). One week after Dox withdrawal, VEGF-A expression returned to baseline (Figure 1C), and remarkably, islet morphology and vascularization normalized over 6 weeks after removal of the VEGF-A stimulus (Figures 1D–1F and S1D). The inverse relationship between  $\beta$  cells and intra-islet ECs during the induction and withdrawal of the VEGF-A stimulus is shown in Figures 1G and 1H.

Six weeks after Dox withdrawal, the regenerated  $\beta$ VEGF-A islets were functionally indistinguishable from No Dox controls (Figure 1I).  $\beta$ VEGF-A mice maintained normal glucose clearance, random blood glucose levels, and body weight during the brief 1 week Dox treatment and subsequent 6 week period of Dox withdrawal (Figures 1J, 1K, S1E, and S1F). This was expected, since 1 week Dox treatment resulted in a partial (~45%)  $\beta$  cell loss, as indicated by total pancreatic insulin content (Figure 1L) and  $\beta$  cell mass measurements (Figure S1G) (Peshavaria et al., 2006). This  $\beta$  cell loss occurred through upregulation of the apoptotic pathway (Figure S2) with an increased number of  $\beta$  cells positive for gamma-phosphorylated histone H2AX (pH2AX), an apoptotic marker of double-stranded DNA breaks, 1 week after Dox (Figures 1M and S2A) (Lu et al., 2006; Ward et al., 2008). Pancreatic glucagon was unchanged 1 week after Dox and during the 6 week period of Dox withdrawal (Figure S1H). The phenotype of  $\beta$ VEGF-A islets was exacerbated with prolonged VEGF-A induction (Figures S1I–S1L). Dox treatment for 3 weeks in  $\beta$ VEGF-A mice led to glucose intolerance, increased fasting glucose levels, and an 80% reduction in total pancreatic insulin content, with ~60% recovery 8 weeks after Dox withdrawal (Figures S1J–S1L). Prolonged Dox administra-

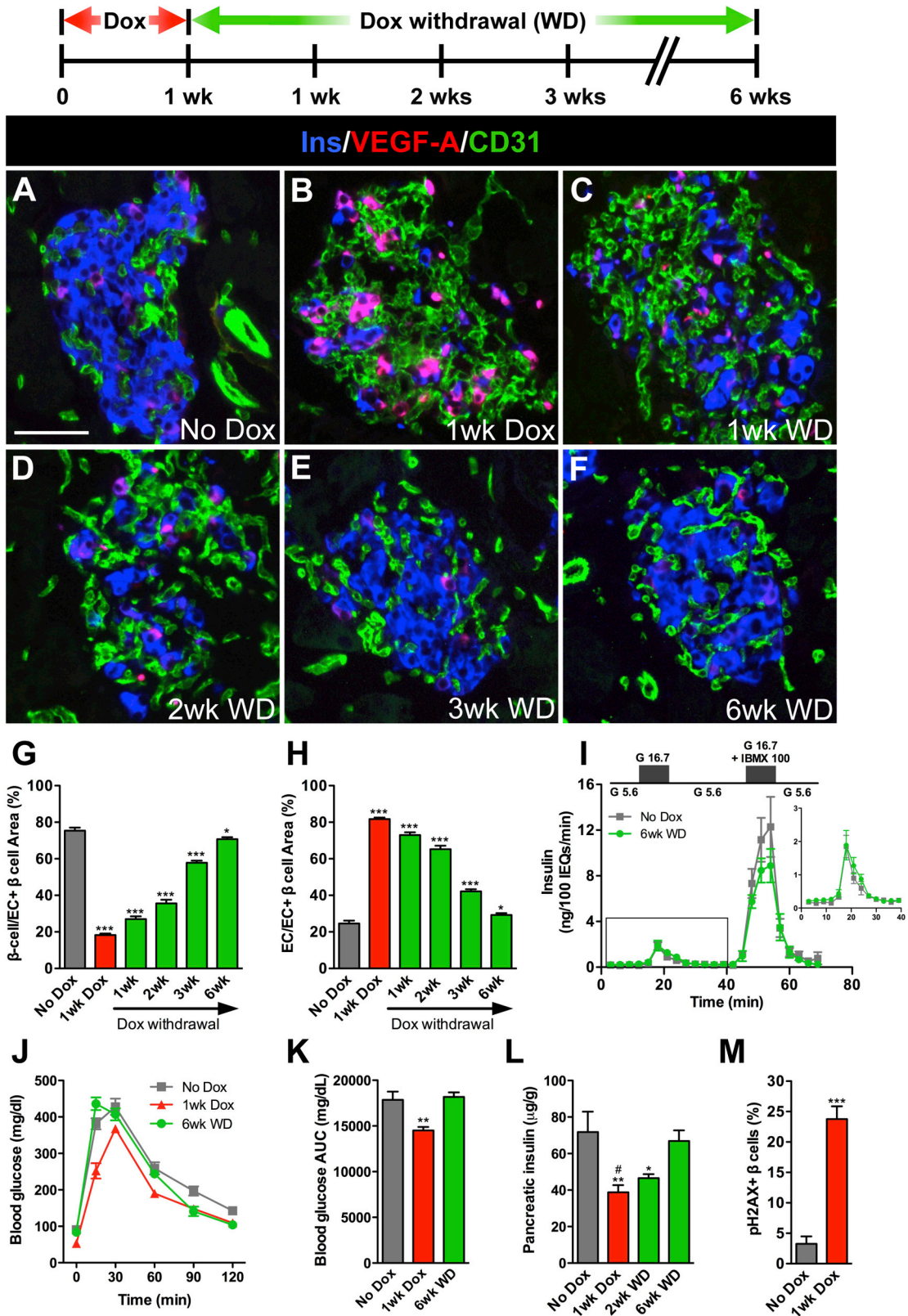
tion (3 weeks) alone was not detrimental to glucose homeostasis, islet, or EC morphology (Figures S3C–S3H).

Dox treatment for 1–3 weeks resulted in VEGF-A overexpression in ~65% of  $\beta$  cells (Figures 1B and S1M). We did note a very slight elevation in basal VEGF-A expression in  $\beta$ VEGF-A mice (Figures 1A and S1A), which caused a modest increase in ECs adjacent to  $\beta$  cells with elevated VEGF-A expression (2%–5%  $\beta$  cells). However, glucose clearance in  $\beta$ VEGF-A mice before Dox administration was identical to both monotransgenic and WT mice (Figures S1J, S1K, S3G, and S3H and data not shown). Although islet vasculature became greatly disorganized with prolonged VEGF-A induction, blood vessels in adjacent exocrine tissue remained normal (Figure S1N), which is consistent with the short-range effect of heparin-bound VEGF-A<sup>164</sup> observed in other vascular beds (Carmeliet and Tessier-Lavigne, 2005). Intravital labeling with endothelium-binding lectin-FITC revealed that even after 3 weeks of persistent VEGF-A overexpression, the majority of intra-islet capillaries were still perfused and functional (Figures S1N and S1O) and lined by a thin layer of laminin+vascular basement membrane (Figures S3A and S3B). We conducted the remainder of our studies on  $\beta$  cell loss and regeneration using a 1 week Dox administration and 6 week Dox withdrawal paradigm to avoid any influence of hyperglycemia.

### Withdrawal of the VEGF-A Stimulus Results in Increased Proliferation of Pre-existing $\beta$ Cells

To define the time course of  $\beta$  cell regeneration in this model, we first followed  $\beta$  cell proliferation in the  $\beta$ VEGF-A pancreas during the course of induction and withdrawal of the VEGF-A stimulus. One week after Dox treatment, intra-islet ECs were highly proliferative, while  $\beta$  cell proliferation decreased below basal level (Figures 2A, 2B, and 2G). This Ki67 labeling pattern was reversed 1 week after Dox withdrawal when ECs begin to subside and  $\beta$  cells proliferate (Figures 2C and 2G). The burst in  $\beta$  cell proliferation was transient and peaked within 2 weeks after Dox withdrawal (Figures 2D–2G). The same temporal profile of  $\beta$  cell replication was seen using BrdU (Figure S3I). Additionally, during 1 week Dox and 6 week recovery phases, the expression pattern of transcription factor Pdx1, known to be expressed in progenitor cells of the developing pancreas, did not differ from No Dox control (Figure S4B), monotransgenic, or WT mice (data not shown). The number of  $\beta$  cells expressing the maturation marker MafA decreased after 1 week Dox treatment, but gradually recovered during 6 weeks of Dox withdrawal (Figures S4C and S4D).

Previous reports indicated that  $\beta$  cell proliferation in the regenerative phase after STZ-mediated injury is dependent on re-expression of polycomb group proteins Bmi-1 and Ezh2 that modify chromatin structure at the *Ink4a/Arf* locus and control  $\beta$  cell growth (Chen et al., 2009; Dhawan et al., 2009). To determine if a similar mechanism was responsible for  $\beta$  cell proliferation in  $\beta$ VEGF-A islets, we labeled pancreatic sections for Bmi-1 (Figures 2H–2K). Although nearly all  $\beta$  cells were Bmi-1+ in No Dox controls at postnatal day 21 (Figure 2H), we did not detect Bmi-1 in  $\beta$  cells of adult  $\beta$ VEGF-A mice 1 or 2 weeks after Dox withdrawal when  $\beta$  cell proliferation reached a maximum (Figures 2J and 2K). These data suggest that the mechanism of  $\beta$  cell proliferation in regenerating  $\beta$ VEGF-A islets differs from the STZ injury model.



(legend on next page)

To further examine the cellular origin of regenerating  $\beta$  cells in this model, we utilized genetic lineage tracing by introducing Pdx1<sup>PB</sup>-CreER<sup>Tm</sup> and R26R<sup>lacZ</sup> components into the  $\beta$ VEGF-A system.  $\beta$  cells were genetically labeled with a  $\beta$ -galactosidase ( $\beta$ -gal) reporter using  $3 \times 1$  mg tamoxifen (Tm) prior to the onset of Dox treatment. We showed previously that this Tm dose effectively induces Cre-loxP recombination in 30% of  $\beta$  cells without undesirable long-lasting residual recombination effects following Tm administration (Reinert et al., 2012). A similar  $\beta$  cell recombination rate was achieved when the Pdx1<sup>PB</sup>-CreER<sup>Tm</sup>;R26R<sup>lacZ</sup> lineage tracing system was incorporated into the  $\beta$ VEGF-A background and was sustained after induction and withdrawal of the VEGF-A stimulus (Figures 3A–3E). As previously reported,  $\beta$ -gal+Ins<sup>-</sup> cells were very rare using the Pdx1<sup>PB</sup>-CreER<sup>Tm</sup> transgenic line (<1%–3% islet non- $\beta$  cells) (Reinert et al., 2012; Zhang et al., 2005). Consistent with the  $\beta$  cell recombination rate,  $\sim$ 30% of Ki67+  $\beta$  cells carried the  $\beta$ -gal reporter 2 weeks after Dox withdrawal (Figures 3F and 3G). Maintaining this steady proportion of  $\beta$ -gal+  $\beta$  cells throughout the time course indicates that new  $\beta$  cells in  $\beta$ VEGF-A mice arise by replication from pre-existing  $\beta$  cells and that the loss of insulin+ cells 1 week after Dox (Figures 1B and 3B) is the result of  $\beta$  cell death and not the loss of insulin labeling or  $\beta$  cell dedifferentiation.

### $\beta$ Cell Replication after VEGF-A Normalization Is Independent of the Pancreatic Site and Soluble Circulating Factors and Is Not Limited to Murine $\beta$ Cells

We next sought to determine whether  $\beta$  cell proliferation in regenerating  $\beta$ VEGF-A islets required the pancreatic location and/or was dependent on soluble circulating factor(s). We also wanted to know whether the factor(s) responsible for this murine  $\beta$  cell proliferation were capable of inducing proliferation in human  $\beta$  cells. To address these questions, we used an islet transplantation model where handpicked WT and  $\beta$ VEGF-A islets were transplanted beneath contralateral kidney capsules of  $\beta$ VEGF-A mice, or alternatively, mixtures with equal amounts of human and WT or  $\beta$ VEGF-A islets were transplanted beneath contralateral kidney capsules of immunodeficient NOD-*scid-IL2r $\gamma$ <sup>null</sup>* mice (Figure 4A). All human islets (HI) used in these experiments demonstrated a robust insulin secretory response to glucose, and this response was further augmented by cAMP potentiation (Figure S5H) (Dai et al., 2012). Transplanted islets were allowed to engraft for 2 weeks, and then the tissues were analyzed at baseline without Dox, 1 week after Dox treatment,

and 2 weeks after Dox withdrawal (Figure 4A). After 1 week of Dox treatment, VEGF-A was induced as effectively in  $\beta$ VEGF-A islet grafts (Figure S5E) as in native  $\beta$ VEGF-A islets (Figure 1B), with both sites showing an extensive increase in EC mass and  $\beta$  cell loss (Figures S5E and S5J). We noted that 1 week after VEGF-A induction, ECs were assembled into multiple layers (Figures 1B, S5E, and S5J). This was followed by a gradual rearrangement in endothelial and islet cells as ECs transitioned to a more single-layered organization 2 weeks after Dox withdrawal (Figures 1D, S5G, and S5L). Similar changes in graft morphology were observed in  $\beta$ VEGF-A grafts both with and without human islets (Figures S5E, S5G, S5J, and S5L). Increased VEGF-A production in  $\beta$ VEGF-A islet grafts and native  $\beta$ VEGF-A islets had no effect on the vascularization of WT islet grafts in contralateral kidneys (Figures S5D, S5F, S5I, and S5K) or the kidney cortex adjacent to  $\beta$ VEGF-A islet grafts (data not shown), pointing again to the localized effect of VEGF-A<sup>164</sup>.

We next measured  $\beta$  cell proliferation rates in WT and  $\beta$ VEGF-A islet grafts at No Dox, 1 week after Dox treatment, and 2 weeks after Dox withdrawal (Figures 4B–4D) when  $\beta$  cell proliferation was maximal in native  $\beta$ VEGF-A islets (Figure 2G). As expected, the  $\beta$  cell proliferation rate was similar in WT and  $\beta$ VEGF-A islet grafts at No Dox and 1 week after Dox treatment (Figure 4D). This low proliferation rate continued in WT islet grafts 2 weeks after Dox withdrawal ( $1.3 \pm 0.2\%$ ), but the  $\beta$  cell replication index in  $\beta$ VEGF-A islet grafts increased  $\sim$ 4-fold ( $4.2 \pm 0.8\%$ ) and was comparable to that in native  $\beta$ VEGF-A islets ( $6.2 \pm 0.7\%$ ). Similarly, 2 weeks after Dox withdrawal, the proliferation rate of human  $\beta$  cells in  $\beta$ VEGF-A + HI grafts was 3-fold higher ( $0.95 \pm 0.18\%$ ) than in WT+HI grafts ( $0.35 \pm 0.07\%$ ) (Figures 4E–4G). Collectively, these data indicate that  $\beta$  cell replication in regenerating  $\beta$ VEGF-A islets is modulated by the local microenvironment independently of the pancreatic site and systemic soluble factors. Furthermore, the factor(s) responsible for  $\beta$  cell proliferation in  $\beta$ VEGF-A islets also promote significant proliferation of human  $\beta$  cells.

### Recruited M $\phi$ s Are Crucial for the $\beta$ Cell Proliferative Response in $\beta$ VEGF-A Islets

Since VEGF-A is known to stimulate the migration of circulating monocytes (Barleon et al., 1996), and  $\beta$  cell proliferation was modulated by the local microenvironment created by increased VEGF-A expression, we sought to determine whether circulating monocytes homed to  $\beta$ VEGF-A islets upon VEGF-A induction and contributed to the  $\beta$  cell proliferative response.

### Figure 1. Increasing $\beta$ Cell VEGF-A Production Increases Intra-Islet ECs but Leads to $\beta$ Cell Loss Followed by $\beta$ Cell Regeneration after Withdrawal of the VEGF-A Stimulus

(A–M) VEGF-A was induced for 1 week (wk) by Dox administration followed by 6 weeks of Dox withdrawal (WD). (A–F) Labeling for insulin (Ins, blue), VEGF-A (red), and EC marker CD31 (green). Scale bar is 50  $\mu$ m and applies to (A)–(F). (G and H) Relationship between  $\beta$  cells (G) and intra-islet ECs (H) upon induction and withdrawal of the VEGF-A stimulus. \*\*\* $p < 0.001$ , 1 week Dox, 1 week WD, 2 week WD, or 3 week WD versus No Dox control; \* $p < 0.05$ , 6 week WD versus No Dox control;  $n = 4$  mice/time point. Islet size measured by pixel area increased slightly but not significantly with intra-islet EC expansion; No Dox,  $6545 \pm 1687$  pixels; 1 week Dox,  $10705 \pm 1712$  pixels,  $p = 0.1939$ . (I) Islets isolated from No Dox controls and at 6 week WD ( $n = 4$  mice/group) were examined in a cell perfusion system. Both groups had normal basal insulin secretion at 5.6 mM glucose (G 5.6), and the magnitude of the insulin secretory response was similar when stimulated with either 16.7 mM glucose (G 16.7;  $9.6 \pm 2.1$  versus  $11.3 \pm 2.5$  ng/100 IEQ,  $p = 0.63$ ) or 16.7 mM glucose + 100  $\mu$ M IBMX (G 16.7 + IBMX 100;  $111 \pm 22$  versus  $84 \pm 13$  ng/100 IEQ,  $p = 0.34$ ). Inset shows enlarged boxed portion of insulin secretory profile. (J and K) Glucose clearance in  $\beta$ VEGF-A mice. \*\* $p < 0.01$ , 1 week Dox ( $n = 10$ ) versus No Dox ( $n = 14$ ) or 6 week WD ( $n = 5$ ). (L) Loss in pancreatic insulin content 1 week after VEGF-A induction was restored over the 6 weeks following Dox withdrawal. \*\* $p < 0.01$ , 1 week Dox versus No Dox; \* $p < 0.05$ , 2 week WD versus No Dox; #,  $p < 0.05$ , 1 week Dox versus 6 week WD; No Dox versus 6 week WD was not statistically significant;  $n = 6$ –7 mice/time point. (M) Increased  $\beta$  cell apoptosis 1 week after VEGF-A induction;  $n = 4$  mice/time point; 100–500  $\beta$  cells analyzed/mouse. \*\*\* $p < 0.001$ , 1 week Dox versus No Dox. Data are shown as the means  $\pm$  SEM.

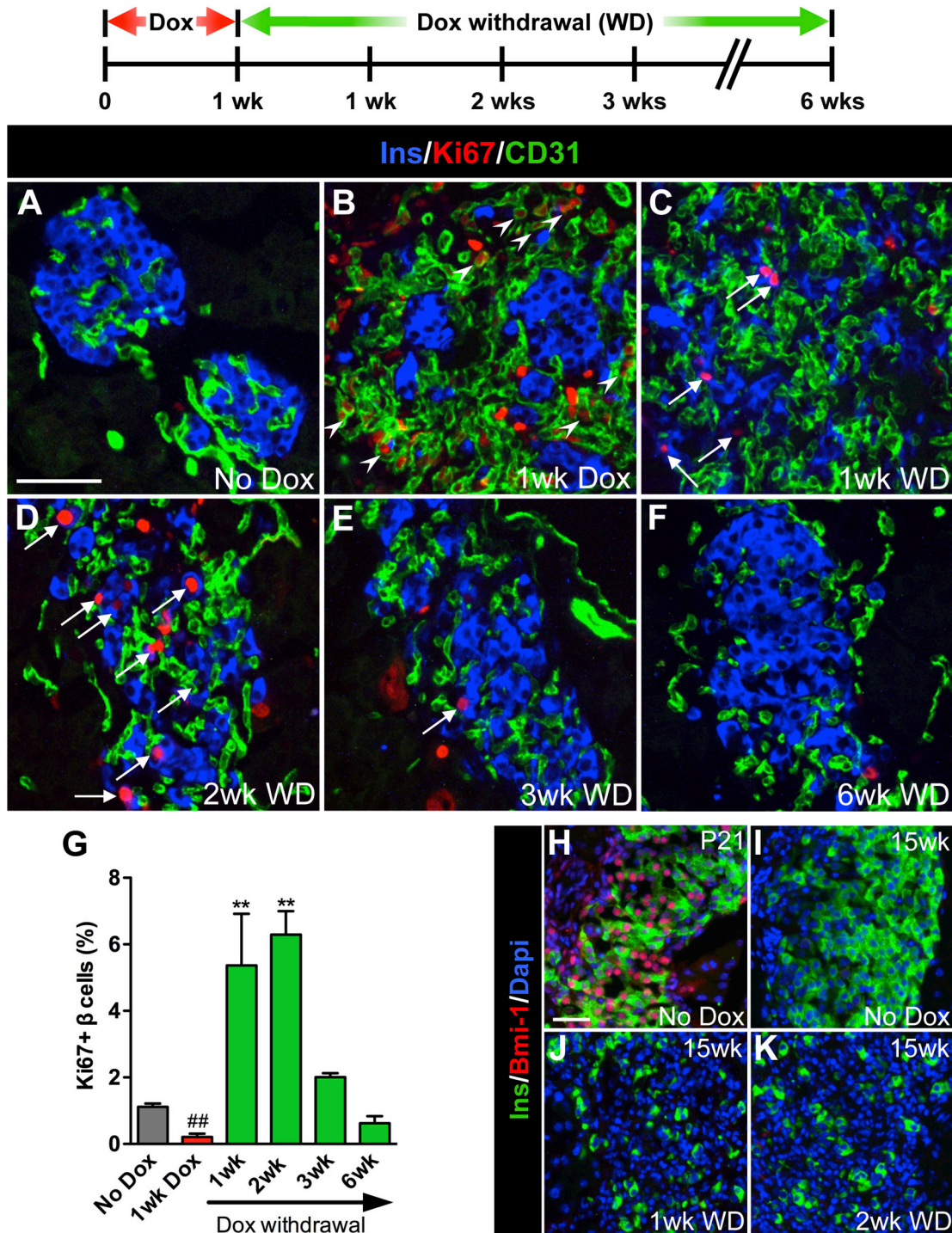


**Figure 2. Removal of the VEGF-A Stimulus Results in a Transient Burst in  $\beta$  Cell Proliferation**

(A–K)  $\beta$  cell proliferation was monitored during the experimental period outlined;  $n = 4$  mice/time point. (A–F) Labeling for insulin (Ins, blue), Ki67 (red), and CD31 (green). Scale bar is 50  $\mu$ m and applies to (A)–(F). (G) Quantification of  $\beta$  cell proliferation. ##,  $p < 0.01$ , 1 week WD versus No Dox, 1 week WD, 2 week WD, or 3 week WD. \*\* $p < 0.01$ , 1 week WD or 2 week WD versus No Dox, 1 week Dox, 3 week WD, or 6 week WD. No Dox, 1 week Dox, 3 week WD, and 6 week WD comparisons were not statistically significant. (H–K) Increased  $\beta$  cell proliferation was not associated with increased Bmi-1; insulin (Ins, green), Bmi-1 (red), Dapi (blue). Scale bar is 25  $\mu$ m and applies to (H)–(K). Data are shown as the means  $\pm$  SEM.

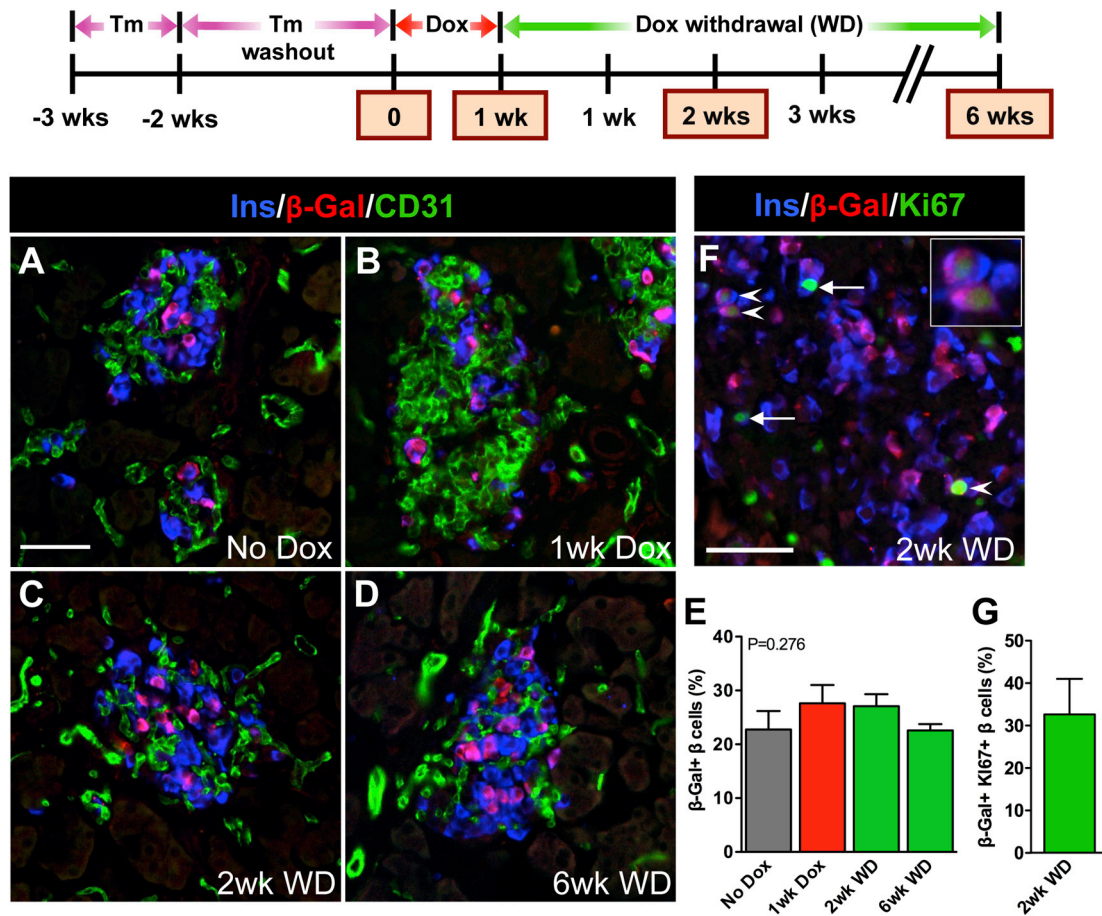


### Figure 3. New $\beta$ Cells in the $\beta$ VEGF-A Model Arise from Replication of Pre-existing $\beta$ Cells

(A–G)  $\beta$  cells in RIP-rtTA;Tet-O-VEGF-A;Pdx1<sup>PB</sup>-CreER<sup>Tm</sup>;R26R<sup>wt/lacZ</sup> transgenic mice were genetically labeled by Tm injection 2 weeks prior to inducing VEGF-A for 1 week by Dox administration followed by 6 weeks of Dox withdrawal. Expression of  $\beta$ -gal in  $\beta$  cells was analyzed in 3–4 mice/time point. (A–D) Labeling for insulin (Ins, blue),  $\beta$ -galactosidase ( $\beta$ -Gal, red), and CD31 (green). Scale bar is 50  $\mu$ m and applies to (A)–(D). (E)  $\beta$ -gal labeling index in  $\beta$  cells was not statistically different at any time point,  $p = 0.2760$ . (F) Genetically labeled  $\beta$  cells proliferate. Arrowheads denote  $\beta$ -gal+Ki67+  $\beta$  cells, progeny of surviving and proliferating  $\beta$  cells (enlargement in inset). Arrows point to  $\beta$ -gal–Ki67+  $\beta$  cells. Scale bar is 50  $\mu$ m. (G) One-third of all proliferating  $\beta$  cells expressed the  $\beta$ -gal genetic mark, which is consistent with genetic labeling in (E). The  $\beta$  cell proliferation index at 2 week WD was  $6.1\% \pm 1.0\%$ , consistent with Figure 2G. Data are shown as the means  $\pm$  SEM.

$\beta$ VEGF-A mice were transplanted with GFP-labeled bone marrow. After bone marrow reconstitution, VEGF-A induction stimulated a marked infiltration of BMCs to the site of  $\beta$  cell injury, and they persisted in islet remnants during the  $\beta$  cell regeneration phase (2 weeks after Dox withdrawal) (Figures 5A–5C). Although GFP+ recruited BMCs were adjacent to  $\beta$  cells and ECs, we did not detect any GFP+/Ins+ cells or GFP+/CD31+ cells. Occasional GFP+ cells were noted around  $\beta$ VEGF-A islets at No Dox (Figures 5A and 5D), but 1 week of VEGF-A induction increased their infiltration nearly 6-fold (Figure S6A). This high level of BMC infiltration into  $\beta$ VEGF-A islets was sustained even 2 weeks after withdrawing the VEGF-A stimulus (Figure S6A), the time point when  $\beta$  cell proliferation is at a maximum. Nearly all GFP+ recruited BMCs expressed the pan-hematopoietic marker CD45 (Figures 5D–5F), and BMC infiltration monitored by CD45 labeling was consistent in mice with or without bone marrow transplantation (data not shown), indicating that the bone marrow transplantation alone did not

enhance the incidence of recruited BMCs in the pancreas and islets. This allowed us to use CD45 as a surrogate marker to follow the BMC infiltration.

Flow cytometry analysis of cells from  $\beta$ VEGF-A islets dispersed after 1 week VEGF-A induction revealed that the vast majority (90%) of CD45+ recruited BMCs were CD11b+ Gr1– M $\Phi$ s (Figure 6A). As monocytes develop into mature M $\Phi$ s, they lose Gr1 expression and increase expression of mature M $\Phi$  markers CD11b and F4/80 (Sharpe et al., 2006). This maturation process is evident in the CD45+ BMC population recruited to  $\beta$ VEGF-A islets where only a few less-mature M $\Phi$ s (CD11b+<sup>Lo</sup>) express F4/80 (3%), while more-mature M $\Phi$ s (CD11b+<sup>Hi</sup>) are much more likely to express F4/80 (60%) (Figure 6B). Labeling tissue sections from mice that received GFP bone marrow transplants with F4/80 confirmed that nearly all GFP+ recruited BMCs in  $\beta$ VEGF-A islets were M $\Phi$ s (Figures S6B–S6D). GFP+ cells expressing the T cell marker CD3 or the B cell marker B220 were very rare (Figures S6E–S6J), and

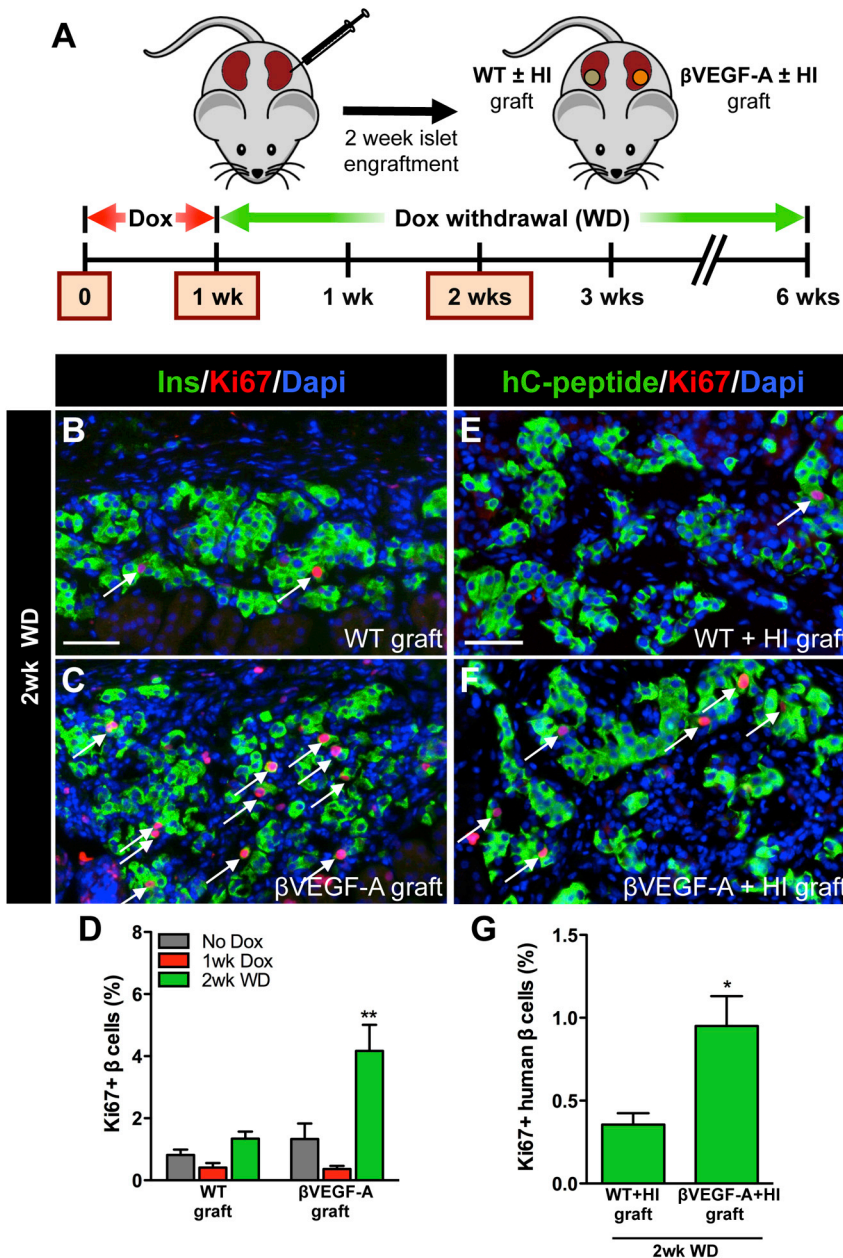


**Figure 4.  $\beta$  Cell Replication Is Independent of the Pancreatic Site and Soluble Circulating Factors and Is Not Limited to Murine  $\beta$  Cells**

(A) Islets from  $\beta$ VEGF-A mice and WT controls were transplanted into  $\beta$ VEGF-A recipients or mixed with human islets (HI) and transplanted into NOD-*scid-IL2r $\gamma^{null}$*  mice. Islets engrafted for 2 weeks then grafts were harvested and analyzed at No Dox, 1 week Dox, and 2 week WD time points; n = 3–4 mice/time point.

(B and C)  $\beta$  cell proliferation at 2 week WD in WT and  $\beta$ VEGF-A islet grafts; insulin (Ins, green), Ki67 (red), and Dapi (blue). Scale bar is 50  $\mu$ m and applies to (B) and (C).

(D) Quantification of  $\beta$  cell proliferation in WT and  $\beta$ VEGF-A islet grafts. \*\*p < 0.01, 2 week WD versus No Dox and 1 week Dox across graft types.

(E and F)  $\beta$  cell proliferation at 2 week WD in WT+HI and  $\beta$ VEGF-A+HI grafts; human C-peptide (hC-peptide, green), Ki67 (red), and Dapi (blue). Scale bar is 50  $\mu$ m and applies to (E) and (F).

(G) Quantification of  $\beta$  cell proliferation in WT+HI and  $\beta$ VEGF-A+HI grafts at 2 week WD. \*p < 0.05. Data are shown as the means  $\pm$  SEM.

chloroacetate esterase staining demonstrated that VEGF-A induction does not lead to neutrophil accumulation (Figures S6K and S6L).

Together, these data indicate that upon VEGF-A induction, circulating monocytes migrate to  $\beta$ VEGF-A islets and differentiate into a mature population of recruited M $\Phi$ s that remain in the islets 2 weeks after the VEGF-A stimulus is withdrawn. In contrast, CD45+ cells were extremely rare in islet remnants after STZ-mediated  $\beta$  cell ablation, and  $\beta$  cell recovery was limited, as indicated by persistent hyperglycemia 6 weeks after STZ treatment (data not shown).

The pattern of CD45 labeling in  $\beta$ VEGF-A islet grafts was similar to native  $\beta$ VEGF-A islets. VEGF-A induction led to the infiltration of CD45+ cells into  $\beta$ VEGF-A islet grafts, and they

persisted within the grafts 2 weeks after VEGF-A stimulus withdrawal, while the population of CD3+ and B220+ cells remained extremely low (data not shown). The incidence of CD45+ cells within WT islet grafts remained low at all three time points with the rare presence of T and B cells (data not shown). Some CD45+ cells were detected around the periphery of islet grafts regardless of the islet genotype and VEGF-A induction, which could be due to the islet transplantation procedure and engraftment process being incompletely resolved. Also, VEGF-A production is increased in isolated islets as a result of hypoxia (Vasir et al., 2001), which alone could stimulate some recruitment of CD45+ cells even in WT islet grafts. Importantly, the infiltration of CD45+ cells was consistently observed only in  $\beta$ VEGF-A islets and  $\beta$ VEGF-A islet grafts

after VEGF-A induction (Figure 5, and data not shown). Similar to native  $\beta$ VEGF-A islets, the majority of CD45+ cells in  $\beta$ VEGF-A grafts were F4/80+ M $\Phi$ s (data not shown). In contrast, F4/80+ cells were rare within WT islet grafts (data not shown).

To determine whether these recruited M $\Phi$ s contribute to the  $\beta$  cell proliferative response during regeneration, we blocked recruitment of M $\Phi$ s to  $\beta$ VEGF-A islets by partial bone marrow ablation (5 Gy irradiation). This methodology has been widely used for M $\Phi$  inactivation (Diamond and Pesek-Diamond, 1991; Ricardo et al., 2008; Wang et al., 2011), and prior studies have shown that 5 Gy irradiation alone neither inhibits nor promotes  $\beta$  cell proliferation (Nakayama et al., 2009; Urbán et al., 2008). Immediately after receiving 5 Gy irradiation,

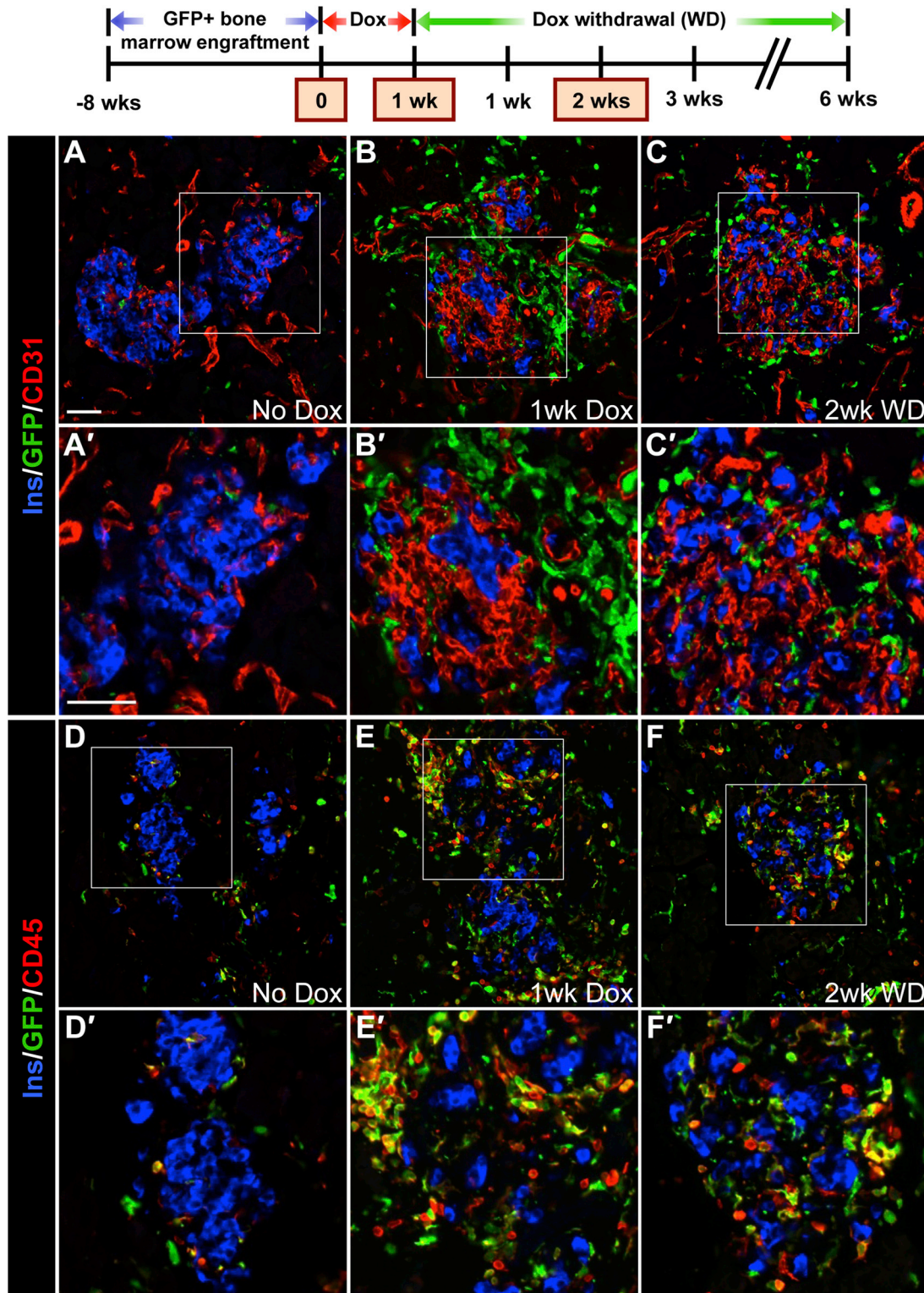


**Figure 5. CD45<sup>+</sup> BMCs Are Recruited to the Site of  $\beta$  Cell Injury upon VEGF-A Induction and Persist in Islet Remnants during  $\beta$  Cell Regeneration**

(A–F)  $\beta$ VEGF-A mice were transplanted with GFP+ bone marrow, and 8 weeks later VEGF-A was induced for 1 week by Dox administration followed by 2 weeks of Dox withdrawal; n = 4–6 mice/time point. (A–C) Labeling for insulin (Ins, blue), CD31 (red) and GFP (green). (D–F) Labeling for insulin (Ins, blue), pan-hematopoietic marker CD45 (red) and GFP (green). Boxes in (A)–(F) denote enlargements in (A')–(F'). Scale bar in (A) is 50  $\mu$ m and applies to (A)–(F). Scale bar in (A') is 50  $\mu$ m and applies to (A')–(F').



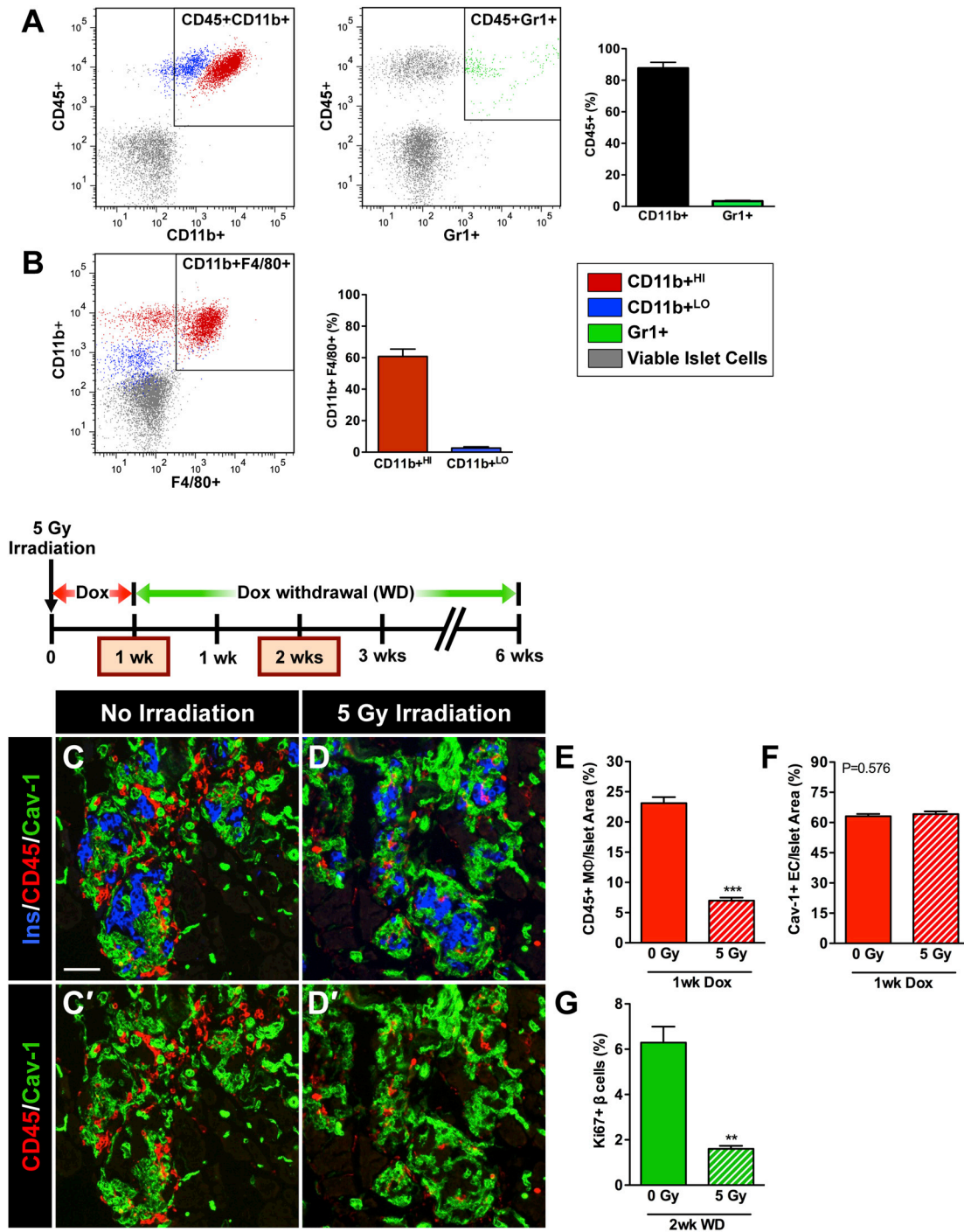


**Figure 6. Recruitment of MΦs into  $\beta$ VEGF-A Islets upon VEGF-A Induction Is Necessary for the  $\beta$  Cell Proliferative Response**

(A and B) Flow cytometry analysis of  $\beta$ VEGF-A islets after 1 week Dox treatment. (A) The CD45+ BMC population recruited to  $\beta$ VEGF-A islets was composed of 90% CD11b+ MΦs and 3% Gr1+ cells. (B) F4/80 expression in subsets of more mature CD11b+<sup>HI</sup> (60%) and less mature CD11b+<sup>LO</sup> (3%) MΦs; n = 5 islet preparations (1–2 mice/preparation).

(C–G) Partial bone marrow ablation prior to VEGF-A induction blocks MΦ recruitment and prevents  $\beta$  cell proliferation. (C and D) Immediately after sublethal irradiation, VEGF-A expression in  $\beta$ VEGF-A mice was induced for 1 week by Dox administration, and tissues were examined for the presence of CD45+ MΦs at 1 week Dox and compared with nonirradiated controls; n = 4 mice/group; insulin (Ins, blue), CD45 (red), and EC marker caveolin-1 (Cav-1, green). (C') and (D') show CD45 (red) and caveolin-1 (green) labeling. Scale bar is 50  $\mu$ m and applies to (C)–(D'). (E) Sublethal irradiation reduced infiltration of CD45+ MΦs, \*\*\*p < 0.001, 0 Gy versus 5 Gy. (F) Sublethal irradiation did not affect intra-islet EC expansion, p = 0.5760, 0 Gy versus 5 Gy. (G) Two weeks after Dox withdrawal,  $\beta$  cell proliferation was significantly reduced in sublethally irradiated  $\beta$ VEGF-A mice versus nonirradiated controls, \*\*p < 0.01; n = 4 mice/group. Data are shown as the means  $\pm$  SEM.

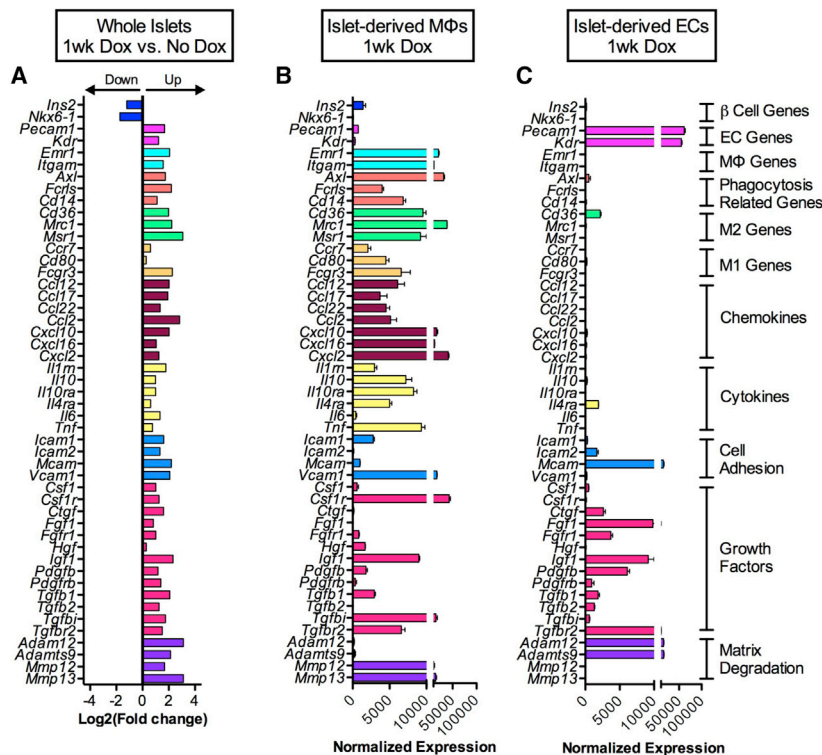


**Figure 7. Transcriptome Analysis of  $\beta$ VEGF-A Islets and Purified Islet-Derived MΦs and ECs**

(A–C) Gene expression profile of whole  $\beta$ VEGF-A islets, islet-derived MΦs, and islet-derived ECs by RNA-Seq; n = 3 replicates/each sample set. (A) Differential expression of  $\beta$  cell-, EC-, and MΦ-specific genes, phagocytosis-related genes, MΦ phenotype markers (M1, classical; M2, alternative), chemokines, cytokines, cell adhesion molecules, growth factors, and matrix degrading enzymes between islets at 1 week Dox versus No Dox,  $p < 0.05$  for fold change  $\geq 2$ . See also data in Figure S6M. (B) At 1 week Dox, recruited MΦs are highly enriched for transcripts of phagocytosis-related genes, M2 markers, chemokines, cytokines, cell adhesion molecules, and metalloproteinases involved in tissue repair. (C) Intra-islet ECs mainly express growth factors and matrix degrading enzymes that facilitate growth factor release from the extracellular matrix. Data in (B) and (C) are plotted as mean  $\pm$  SEM. (D) Paradigm for the role of MΦ-EC interactions in  $\beta$  cell regeneration. Upon VEGF-A induction, intra-islet ECs proliferate and circulating monocytes recruited to islets differentiate into MΦs. These CD45+CD11b+Gr1- recruited MΦs and ECs produce effector molecules that either directly or cooperatively induce  $\beta$  cell proliferation and regeneration. Data are shown as the means  $\pm$  SEM.

**Both MΦs and ECs in the  $\beta$ VEGF-A Islet Microenvironment Produce Factors that Promote Tissue Repair/Regeneration**

Tissue regeneration is a multistep process that is mediated by complex interactions between multiple cell types (Nucera et al., 2011). Because recruited MΦs and intra-islet ECs are two major components of the  $\beta$ VEGF-A islet microenvironment at the onset of  $\beta$  cell regeneration, we postulated that MΦs produce effector molecules that induce  $\beta$  cell proliferation/regeneration either directly or in concert with intra-islet ECs. To identify the components and cellular sources of intra-islet signaling at the onset of  $\beta$  cell proliferation, we performed transcriptome analysis of whole  $\beta$ VEGF-A islets isolated at No Dox and 1 week after VEGF-A induction, when

$\beta$ VEGF-A mice began 1 week Dox treatment. The partial bone marrow ablation significantly reduced infiltration of CD45+ MΦs to  $\beta$ VEGF-A-overexpressing islets (Figures 6C–6E). In spite of the greatly reduced MΦ population, intra-islet ECs continued to expand, resulting in  $\beta$  cell loss (Figure 6F). However, subsequent measurement of the Ki67 labeling index in  $\beta$  cells 2 weeks after Dox withdrawal showed reduced MΦ infiltration into  $\beta$ VEGF-A islets resulting in an  $\sim 3$ -fold decrease in  $\beta$  cell proliferation (Figure 6G). These results suggest that recruited MΦs support  $\beta$  cell proliferation following islet injury.

both ECs and MΦs are most abundant in islets, and compared their transcriptional profiles to purified islet-derived MΦs and ECs (Figures 7A–7C and S7). Our data revealed that some factors are unique to individual cell types and some are shared by MΦs and ECs. For example, after 1 week VEGF-A induction, recruited MΦs were highly enriched for transcripts of phagocytosis-related genes (*Axl*, *Fcrls*, *Cd14*), markers of alternatively activated MΦs (M2) (*Cd36*, *Mrc1*, *Msr1*), some markers of classically activated MΦs (M1) (*Ccr7*, *Cd80*, *Fcgr3*), chemokines (*Ccl12*, *Ccl2*, *Cxcl10*, *Cxcl2*), cytokines (*Il10*, *Il10ra*, *Il4ra*, *Tnf*), cell adhesion molecules (*Icam1*, *Vcam1*), metalloproteinases

(MMPs) involved in tissue repair (*Mmp12*, *Mmp13*), and some growth factors (*Hgf*, *Igf1*, *Pdgfb*, *Tgfb1*, *Tgfb2*) (Figure 7B). In contrast, intra-islet ECs mainly expressed growth factors (*Ctgf*, *Fgf1*, *Igf1*, *Pdgfb*) and matrix-degrading enzymes (*Adam12*, *Adamts9*) that facilitate growth factor release from the extracellular matrix (Figure 7C) (Apte, 2009; Kveiborg et al., 2008). Additionally, our data indicate that intra-islet ECs produce factors (*Tgfb* family; including *Tgfb1*, *Tgfb2*) and cell adhesion molecules (*Icam2*, *Mcam*) directly involved in monocyte recruitment and M2 M $\Phi$  activation (Bardin et al., 2009; Ricardo et al., 2008; Tsunawaki et al., 1988). These data provide strong evidence for a model of  $\beta$  cell regeneration where factors produced by both recruited M $\Phi$ s and intra-islet ECs create a microenvironment that promotes  $\beta$  cell proliferation (Figure 7D).

## DISCUSSION

VEGF-A is a master regulator of islet vascular patterning, microvascular permeability, and function, but the role of the VEGF-A signaling pathway and intra-islet ECs in regulating  $\beta$  cell mass is incompletely understood. Here we used a model of inducible and reversible  $\beta$  cell-specific VEGF-A overexpression to investigate how VEGF-A signaling modulates intra-islet vasculature, islet microenvironment, and  $\beta$  cell mass. Increasing intra-islet ECs by transient VEGF-A induction surprisingly led to reduced, not increased,  $\beta$  cell mass. However, withdrawal of the VEGF-A stimulus created a local microenvironment that promoted robust  $\beta$  cell proliferation, with restoration of  $\beta$  cell mass, islet architecture, and vascularization. This proliferation, which was independent of the pancreatic environment or systemic factors, required recruitment of M $\Phi$ s to the site of islet regeneration. Based on these findings, we propose a mechanism to induce  $\beta$  cell regeneration involving recruited M $\Phi$ s and intra-islet ECs (discussed below).

Transiently increased VEGF-A production in adult  $\beta$  cells in our model resembled recently described restrictive effects of hypervascularization on pancreatic epithelial branching, endocrine cell differentiation, and  $\beta$  cell mass (Agudo et al., 2012; Cai et al., 2012; Magenheimer et al., 2011; Sand et al., 2011) and contrasted with previously reported islet hyperplasia in a Pdx1-VEGF-A transgenic model (Lammert et al., 2001). Similar deleterious effects of VEGF-A-induced neovascularization were observed previously in liver and heart (Grunewald et al., 2006). In our study, a significant decrease in  $\beta$  cell proliferation and mass and increased apoptosis were observed when intra-islet ECs became proliferative. It is possible that activated ECs produce factors causing  $\beta$  cell loss, or  $\beta$  cells regress due to space constraints and perturbed cell-cell contacts within the islet caused by rapid EC outgrowth. Although the expanding islet endothelium became disorganized, it is unlikely that the loss of  $\beta$  cells was caused by lack of blood flow or hemorrhage, since islet vasculature was perfused as shown by labeling with endothelium-binding lectin (Brissova et al., 2006). Determining the exact cause(s) of  $\beta$  cell death will require additional investigation. Taken together, we show that precise control of VEGF-A production in adult  $\beta$  cells is crucial for islet vascular homeostasis and maintenance of normal  $\beta$  cell mass. This is important for efforts to utilize ECs in embryonic stem cell differentiation protocols or to promote islet survival after islet transplantation.

Withdrawal of the VEGF-A stimulus in  $\beta$ VEGF-A islets led to a remarkably rapid recovery of  $\beta$  cells by a transient increase in proliferation. Lineage tracing analysis showed that  $\beta$  cell proliferation from pre-existing  $\beta$  cells was the main mechanism of  $\beta$  cell recovery in the  $\beta$ VEGF-A model. Furthermore, using a transplantation model with WT and  $\beta$ VEGF-A islets transplanted under contralateral kidney capsules, we were able to exclude systemic effects of soluble factors, namely glucose (Porat et al., 2011), and demonstrate conclusively that  $\beta$  cell proliferation following injury was stimulated by signals derived from the local islet milieu. Remarkably, these localized signals were also able to significantly increase human  $\beta$  cell proliferation.

Although  $\beta$  cell proliferation in the  $\beta$ VEGF-A model is independent of systemic soluble factors, we found that islet vascular expansion and  $\beta$  cell loss were accompanied by a dramatic infiltration of CD45+CD11b+Gr1<sup>-</sup> M $\Phi$ s. In addition, our data demonstrate that recruited M $\Phi$ s infiltrating  $\beta$ VEGF-A islets and islet grafts neither incorporate into islet vasculature nor differentiate into insulin-producing cells, but instead remain in close association with  $\beta$  cells and intra-islet ECs. This robust recruitment of M $\Phi$ s is, for example, very distinct from the STZ-mediated model of  $\beta$  cell injury where transplantation of BMCs has an extremely limited effect on  $\beta$  cell recovery and BMCs were mostly found around pancreatic ducts (Hasegawa et al., 2007; Hess et al., 2003). Moreover, when the recruitment of CD45+CD11b+Gr1<sup>-</sup> M $\Phi$ s in our model was blocked by partial bone marrow ablation,  $\beta$  cell proliferation was greatly reduced, suggesting that infiltration of these M $\Phi$ s is crucial for the  $\beta$  cell proliferative response in regenerating  $\beta$ VEGF-A islets. Depending on the microenvironment, M $\Phi$ s can acquire distinct functional phenotypes. Two well-established M $\Phi$  phenotypes are often referred to as classically activated proinflammatory M $\Phi$ s (M1) and alternatively activated M $\Phi$ s (M2) that promote tissue repair/regeneration through phagocytosis, scar tissue digestion, and growth factor secretion and release from the extracellular matrix (Sica and Mantovani, 2012). Transcriptome analysis showed that M $\Phi$ s recruited to  $\beta$ VEGF-A islets express high levels of M2 markers along with MMPs associated with tissue restoration and remodeling, and lower levels of M1 markers, indicating that these M $\Phi$ s likely have a unique regenerative phenotype (Ricardo et al., 2008; Sica and Mantovani, 2012). Very little is known about the role of M $\Phi$ s in adult  $\beta$  cell maintenance, but during late stages of pancreatic development, mice with severe M $\Phi$  deficiency had reduced  $\beta$  cell proliferation,  $\beta$  cell mass, and impaired islet morphogenesis (Banaei-Bouhaleb et al., 2004).

While recruited M $\Phi$ s are present in  $\beta$ VEGF-A islets during VEGF-A induction,  $\beta$  cell proliferation does not begin until 1 week after Dox withdrawal, when intra-islet ECs switch from proliferative angiogenesis to quiescence, suggesting that quiescent intra-islet ECs provide permissive or instructive signals for the  $\beta$  cell regenerative process. These islet-derived ECs produce several modulators of cell proliferation and also secrete factors that direct M2 M $\Phi$  activation (He et al., 2012; Tsunawaki et al., 1988). Recent work from several groups suggests that organ-specific vascular niches and VEGF-A-VEGFR2 signaling are major determinants in organ repair and tumorigenesis where ECs produce tissue-specific paracrine growth factors, termed angiocrine factors (Butler et al., 2010a). For example, during liver regeneration, sinusoidal ECs provide the vascular niche required

to initiate hepatic proliferation by producing angiocrine factors such as HGF and Wnt2 (Ding et al., 2010). In bone marrow, stress-induced expression of Notch ligands by sinusoidal ECs is necessary for hematopoietic stem cell reconstitution (Butler et al., 2010b). After a partial lung ablation, pulmonary capillary ECs stimulate proliferation of epithelial progenitor cells through processes involving VEGFR2 and FGFR1 activation and production of MMP14 (Ding et al., 2011). Furthermore, production of angiocrine factors by tumor vessels directly leads to tumor progression (Butler et al., 2010a). In the pancreas, VEGF-A-VEGFR2 signaling is a principal regulator of islet capillary network formation and maintenance (Brissova et al., 2006; Lammert et al., 2003). In addition, ECs are critical for induction of islet endocrine cell differentiation (Lammert et al., 2001; Yoshitomi and Zaret, 2004), and early loss of ECs in developing islets leads not only to reduced  $\beta$  cell mass at birth but also reduced basal  $\beta$  cell proliferation in the adult (Reinert et al., 2013). Transcriptional profiling of intra-islet ECs suggests that they contribute to  $\beta$  cell regeneration by facilitating monocyte recruitment and M2 M $\Phi$  activation and by producing an array of growth factors and MMPs that increase growth factor bioavailability.

The main challenge of  $\beta$  cell replacement therapy is determining how to generate a sufficient quantity of high-quality mature human  $\beta$  cells. Therefore, understanding mechanisms that modulate  $\beta$  cell regeneration and fostering this process may help rescue remaining  $\beta$  cell mass in type 1 and type 2 diabetes. Based on our findings, we propose a model of  $\beta$  cell regeneration (Figure 7D) where the local islet microenvironment, dynamically modulated by VEGF-A, plays an integral part in the  $\beta$  cell regenerative process. Increased VEGF-A production in adult  $\beta$  cells results in intra-islet EC activation and  $\beta$  cell loss, which demonstrates the essential role of regulated VEGF-A signaling in maintaining islet vascular homeostasis and  $\beta$  cell mass. At the same time, however, islet VEGF-A induction leads to the recruitment of CD45+CD11b+Gr1<sup>-</sup> M $\Phi$ s. After withdrawal of the VEGF-A stimulus, these recruited M2-like M $\Phi$ s persist in islet remnants and produce effector molecules that directly, or in concert with quiescent intra-islet ECs, promote  $\beta$  cell proliferation and regeneration independent of the pancreatic site and systemic factors.

It will be important to further characterize the M $\Phi$ s responsible for the  $\beta$  cell proliferative effect and determine how to promote their recruitment to pancreatic islets. Furthermore, understanding signals derived from the intra-islet endothelium will allow us to define the mechanism by which these recruited M $\Phi$ s promote  $\beta$  cell proliferation and develop them as a potential therapeutic for diabetes.

## EXPERIMENTAL PROCEDURES

### Mouse Models

Bitransgenic mice with Dox-inducible  $\beta$  cell-specific overexpression of human VEGF-A<sup>164</sup> were generated by crossing RIP-rTA male mice and Tet-O-VEGF-A female mice, both on a C57BL/6 background (Efrat et al., 1995; Ohno-Matsui et al., 2002). Mice for lineage tracing analysis were generated by crosses of the Pdx1<sup>fl/fl</sup>-CreER<sup>TM</sup> line (Zhang et al., 2005) and R26R<sup>lacZ/lacZ</sup> reporter strain (Soriano, 1999) with RIP-rTA and Tet-O-VEGF-A transgenic mice. VEGF-A transgene expression was activated in 10- to 12-week-old mice by Dox administration (5 mg/ml) in light-protected drinking water containing 1% Splenda for a period of 1–3 weeks. For lineage tracing analysis,  $\beta$  cells

were genetically marked with  $\beta$ -gal by s.c. Tm injection 2 weeks prior to Dox administration (Reinert et al., 2012). C57BL/6 mice and GFPC57BL/6-Tg(CAG-EGFP)10sb/J mice were obtained from The Jackson Laboratory (Bar Harbor, ME). Human islets were transplanted into immunodeficient NOD-scid-IL2r $\gamma$ <sup>null</sup> mice (King et al., 2008). Genotyping was performed on tail biopsies with primers previously described (Efrat et al., 1995; Ohno-Matsui et al., 2002; Soriano, 1999; Zhang et al., 2005). All animal studies were approved by the Institutional Animal Care and Use Committee at Vanderbilt University Medical Center.

### Islet Isolation and Transplantation

Islets were isolated by intraductal infusion of collagenase P as described (Brissova et al., 2004). WT C57BL/6 and  $\beta$ VEGF-A islets were transplanted under contralateral kidney capsules into  $\beta$ VEGF-A recipients as described (Brissova et al., 2004). Human islets from three donors with an average age of 23 years (range 20–28) and average BMI of 28.7 (range 19.0–33.8) were obtained through the Integrated Islet Distribution Program. Mixtures with equal amounts of human and WT or  $\beta$ VEGF-A islets (100 islet equivalents/per each group) were transplanted beneath contralateral kidney capsules of immunodeficient NOD-scid-IL2r $\gamma$ <sup>null</sup> mice.

### Bone Marrow Isolation and Transplantation

Bone marrow was harvested from cleaned femurs and tibias of 6-week-old GFPC57BL/6-Tg(CAG-EGFP)10sb/J donors (Okabe et al., 1997) by flushing them with RPMI-1640 medium containing 2% fetal bovine serum plus heparin (5 U/ml). Six-week-old  $\beta$ VEGF-A recipients received a single dose of lethal irradiation (9 Gy) followed by injection of  $5 \times 10^6$  bone marrow cells delivered in 200  $\mu$ l of RPMI-1640 media via the retro-orbital sinus. Recipients were treated with 100 mg/l neomycin and 10 mg/l polymyxin B sulfate (X-Gen Pharm) in drinking water beginning 3 days prior to irradiation and continuing for 3 weeks after bone marrow transplantation. Hematopoietic engraftment was assayed 8 weeks after transplantation as well as after 1 week Dox, and 2 weeks after Dox withdrawal by flow cytometry analysis. All animals achieved high hematopoietic chimerism (>80%). Partial bone marrow ablation was achieved with 5 Gy irradiation (Wang et al., 2011).

### Flow Cytometry

Details of the procedures are available in the [Supplemental Experimental Procedures](#).

### Tissue Collection and Immunocytochemistry

Collection of pancreata or kidneys bearing islet transplants and immunocytochemistry were performed as described (Brissova et al., 2006). Details of the procedures are available in the [Supplemental Experimental Procedures](#).

### Glucose Tolerance Testing, Islet Function, and Pancreatic Hormone Content

Methodologies for glucose tolerance testing, islet function, and pancreatic hormone content were previously described (Brissova et al., 2006). Details of the procedures are available in the [Supplemental Experimental Procedures](#).

### RNA Sequencing and Analysis

Details of the procedures are available in the [Supplemental Experimental Procedures](#).

### Statistical Analysis

Unpaired t test and one-way analysis of variance with Newman-Keuls multiple comparison test were used to compare outcomes in mice of different genotypes. Data were expressed as mean  $\pm$  SEM.

### ACCESSION NUMBERS

The data for the transcriptome analysis described in this manuscript have been deposited in NCBI's Gene Expression Omnibus and are available at GEO: GSE72546.

## SUPPLEMENTAL INFORMATION

Supplemental Information includes seven figures, three tables, and Supplemental Experimental Procedures and can be found with this article online at <http://dx.doi.org/10.1016/j.cmet.2014.02.001>.

## ACKNOWLEDGMENTS

We thank Drs. S. Efrat, P. Campochiaro, and M. Gannon for providing mice. We thank C.V.E. Wright and R. Stein for antibody gifts. We are grateful to Drs. P. Kendall, J. Thomas, V. Babaev, A. Hatzopoulos, P. Young, and Y. Dor for helpful discussions. This work was supported by grants from the Department of Veterans Affairs, the NIH (DK66636, DK69603, DK63439, DK62641, DK72473, DK089572, DK09538, DK68764), JDRF, and the Vanderbilt Diabetes Research and Training Center (DK20593). Islet isolation was performed in the Vanderbilt Islet Procurement and Analysis Core (DK20593). Bone marrow isolation and transplantation were performed in the Vanderbilt Cardiovascular Pathophysiology & Complications Core (DK59637). Image acquisition was performed in part through use of the Vanderbilt Cell Imaging Shared Resource (CA68485, DK20593, DK58404, HD15052, DK59637, EY08126). Flow cytometry analysis was performed in the Vanderbilt Flow Cytometry Shared Resource (P30 CA68485, DK058404).

Received: October 12, 2012

Revised: March 5, 2013

Accepted: January 27, 2014

Published: February 20, 2014

## REFERENCES

- Agudo, J., Ayuso, E., Jimenez, V., Casellas, A., Mallol, C., Salavert, A., Tafuro, S., Obach, M., Ruzo, A., Moya, M., et al. (2012). Vascular Endothelial Growth Factor-Mediated Islet Hypervascularization and Inflammation Contribute to Progressive Reduction of  $\beta$ -Cell Mass. *Diabetes* *61*, 2851–2861.
- Apte, S.S. (2009). A disintegrin-like and metalloprotease (reprolysin-type) with thrombospondin type 1 motif (ADAMTS) superfamily: functions and mechanisms. *J. Biol. Chem.* *284*, 31493–31497.
- Banaei-Bouchareb, L., Gouon-Evans, V., Samara-Boustani, D., Castellotti, M.C., Czernichow, P., Pollard, J.W., and Polak, M. (2004). Insulin cell mass is altered in Csf1op/Csf1op macrophage-deficient mice. *J. Leukoc. Biol.* *76*, 359–367.
- Bardin, N., Blot-Chabaud, M., Despoix, N., Kebir, A., Harhour, K., Arsanto, J.-P., Espinosa, L., Perrin, P., Robert, S., Vely, F., et al. (2009). CD146 and its soluble form regulate monocyte transendothelial migration. *Arterioscler. Thromb. Vasc. Biol.* *29*, 746–753.
- Barleon, B., Sozzani, S., Zhou, D., Weich, H.A., Mantovani, A., and Marmé, D. (1996). Migration of human monocytes in response to vascular endothelial growth factor (VEGF) is mediated via the VEGF receptor flt-1. *Blood* *87*, 3336–3343.
- Brissova, M., Fowler, M., Wiebe, P., Shostak, A., Shiota, M., Radhika, A., Lin, P.C., Gannon, M., and Powers, A.C. (2004). Intra-islet endothelial cells contribute to revascularization of transplanted pancreatic islets. *Diabetes* *53*, 1318–1325.
- Brissova, M., Shostak, A., Shiota, M., Wiebe, P.O., Poffenberger, G., Kantz, J., Chen, Z., Carr, C., Jerome, W.G., Chen, J., et al. (2006). Pancreatic islet production of vascular endothelial growth factor—a is essential for islet vascularization, revascularization, and function. *Diabetes* *55*, 2974–2985.
- Butler, J.M., Kobayashi, H., and Raffii, S. (2010a). Instructive role of the vascular niche in promoting tumour growth and tissue repair by angiocrine factors. *Nat. Rev. Cancer* *10*, 138–146.
- Butler, J.M., Nolan, D.J., Vertes, E.L., Varnum-Finney, B., Kobayashi, H., Hooper, A.T., Seandel, M., Shido, K., White, I.A., Kobayashi, M., et al. (2010b). Endothelial cells are essential for the self-renewal and repopulation of Notch-dependent hematopoietic stem cells. *Cell Stem Cell* *6*, 251–264.
- Cai, Q., Brissova, M., Reinert, R.B., Pan, F.C., Brahmachary, P., Jeansson, M., Shostak, A., Radhika, A., Poffenberger, G., Quaggin, S.E., et al. (2012). Enhanced expression of VEGF-A in  $\beta$  cells increases endothelial cell number but impairs islet morphogenesis and  $\beta$  cell proliferation. *Dev. Biol.* *367*, 40–54.
- Carmeliet, P., and Tessier-Lavigne, M. (2005). Common mechanisms of nerve and blood vessel wiring. *Nature* *436*, 193–200.
- Chen, H., Gu, X., Su, I.-H., Bottino, R., Contreras, J.L., Tarakhovskiy, A., and Kim, S.K. (2009). Polycomb protein Ezh2 regulates pancreatic beta-cell Ink4a/Arf expression and regeneration in diabetes mellitus. *Genes Dev.* *23*, 975–985.
- Dai, C., Brissova, M., Hang, Y., Thompson, C., Poffenberger, G., Shostak, A., Chen, Z., Stein, R., and Powers, A.C. (2012). Islet-enriched gene expression and glucose-induced insulin secretion in human and mouse islets. *Diabetologia* *55*, 707–718.
- Dhawan, S., Tschen, S.-I., and Bhushan, A. (2009). Bmi-1 regulates the Ink4a/Arf locus to control pancreatic beta-cell proliferation. *Genes Dev.* *23*, 906–911.
- Diamond, J.R., and Pesek-Diamond, I. (1991). Sublethal X-irradiation during acute puromycin nephrosis prevents late renal injury: role of macrophages. *Am. J. Physiol.* *260*, F779–F786.
- Ding, B.-S., Nolan, D.J., Butler, J.M., James, D., Babazadeh, A.O., Rosenwaks, Z., Mittal, V., Kobayashi, H., Shido, K., Lyden, D., et al. (2010). Inductive angiocrine signals from sinusoidal endothelium are required for liver regeneration. *Nature* *468*, 310–315.
- Ding, B.-S., Nolan, D.J., Guo, P., Babazadeh, A.O., Cao, Z., Rosenwaks, Z., Crystal, R.G., Simons, M., Sato, T.N., Worgall, S., et al. (2011). Endothelial-derived angiocrine signals induce and sustain regenerative lung alveolarization. *Cell* *147*, 539–553.
- Efrat, S., Fusco-DeMane, D., Lemberg, H., al Emran, O., and Wang, X. (1995). Conditional transformation of a pancreatic beta-cell line derived from transgenic mice expressing a tetracycline-regulated oncogene. *Proc. Natl. Acad. Sci. USA* *92*, 3576–3580.
- Grunewald, M., Avraham, I., Dor, Y., Bachar-Lustig, E., Itin, A., Jung, S., Chimentli, S., Landsman, L., Abramovitch, R., and Keshet, E. (2006). VEGF-induced adult neovascularization: recruitment, retention, and role of accessory cells. *Cell* *124*, 175–189.
- Hasegawa, Y., Ogihara, T., Yamada, T., Ishigaki, Y., Imai, J., Uno, K., Gao, J., Kaneko, K., Ishihara, H., Sasano, H., et al. (2007). Bone marrow (BM) transplantation promotes beta-cell regeneration after acute injury through BM cell mobilization. *Endocrinology* *148*, 2006–2015.
- He, H., Xu, J., Warren, C.M., Duan, D., Li, X., Wu, L., and Iruela-Arispe, M.L. (2012). Endothelial cells provide an instructive niche for the differentiation and functional polarization of M2-like macrophages. *Blood* *120*, 3152–3162.
- Hess, D., Li, L., Martin, M., Sakano, S., Hill, D., Strutt, B., Thyssen, S., Gray, D.A., and Bhatia, M. (2003). Bone marrow-derived stem cells initiate pancreatic regeneration. *Nat. Biotechnol.* *21*, 763–770.
- King, M., Pearson, T., Shultz, L.D., Leif, J., Bottino, R., Trucco, M., Atkinson, M.A., Wasserfall, C., Herold, K.C., Woodland, R.T., et al. (2008). A new HUPBL model for the study of human islet alloreactivity based on NOD-scid mice bearing a targeted mutation in the IL-2 receptor gamma chain gene. *Clin. Immunol.* *126*, 303–314.
- Kveiborg, M., Albrechtsen, R., Couchman, J.R., and Wewer, U.M. (2008). Cellular roles of ADAM12 in health and disease. *Int. J. Biochem. Cell Biol.* *40*, 1685–1702.
- Lammert, E., Cleaver, O., and Melton, D. (2001). Induction of pancreatic differentiation by signals from blood vessels. *Science* *294*, 564–567.
- Lammert, E., Gu, G., McLaughlin, M., Brown, D., Brekken, R., Murtaugh, L.C., Gerber, H.-P., Ferrara, N., and Melton, D.A. (2003). Role of VEGF-A in vascularization of pancreatic islets. *Curr. Biol.* *13*, 1070–1074.
- Lu, C., Zhu, F., Cho, Y.-Y., Tang, F., Zykova, T., Ma, W.-Y., Bode, A.M., and Dong, Z. (2006). Cell apoptosis: requirement of H2AX in DNA ladder formation, but not for the activation of caspase-3. *Mol. Cell* *23*, 121–132.
- Magenheim, J., Illovich, O., Lazarus, A., Klochendler, A., Ziv, O., Werman, R., Hija, A., Cleaver, O., Mishani, E., Keshet, E., and Dor, Y. (2011). Blood vessels restrain pancreas branching, differentiation and growth. *Development* *138*, 4743–4752.

- Nakayama, S., Uchida, T., Choi, J.B., Fujitani, Y., Ogihara, T., Iwashita, N., Azuma, K., Mochizuki, H., Hirose, T., Kawamori, R., et al. (2009). Impact of whole body irradiation and vascular endothelial growth factor-A on increased beta cell mass after bone marrow transplantation in a mouse model of diabetes induced by streptozotocin. *Diabetologia* 52, 115–124.
- Nucera, S., Biziato, D., and De Palma, M. (2011). The interplay between macrophages and angiogenesis in development, tissue injury and regeneration. *Int. J. Dev. Biol.* 55, 495–503.
- Nyman, L.R., Wells, K.S., Head, W.S., McCaughey, M., Ford, E., Brissova, M., Piston, D.W., and Powers, A.C. (2008). Real-time, multidimensional in vivo imaging used to investigate blood flow in mouse pancreatic islets. *J. Clin. Invest.* 118, 3790–3797.
- Ohno-Matsui, K., Hirose, A., Yamamoto, S., Saikia, J., Okamoto, N., Gehlbach, P., Duh, E.J., Hackett, S., Chang, M., Bok, D., et al. (2002). Inducible expression of vascular endothelial growth factor in adult mice causes severe proliferative retinopathy and retinal detachment. *Am. J. Pathol.* 160, 711–719.
- Okabe, M., Ikawa, M., Kominami, K., Nakanishi, T., and Nishimune, Y. (1997). 'Green mice' as a source of ubiquitous green cells. *FEBS Lett.* 407, 313–319.
- Peshavaria, M., Larmie, B.L., Lausier, J., Satish, B., Habibovic, A., Roskens, V., Larock, K., Everill, B., Leahy, J.L., and Jetton, T.L. (2006). Regulation of pancreatic beta-cell regeneration in the normoglycemic 60% partial-pancreatectomy mouse. *Diabetes* 55, 3289–3298.
- Porat, S., Weinberg-Corem, N., Tornovsky-Babaey, S., Schyr-Ben-Haroush, R., Hija, A., Stolovich-Rain, M., Dadon, D., Granot, Z., Ben-Hur, V., White, P., et al. (2011). Control of pancreatic  $\beta$  cell regeneration by glucose metabolism. *Cell Metab.* 13, 440–449.
- Reinert, R.B., Kantz, J., Misfeldt, A.A., Poffenberger, G., Gannon, M., Brissova, M., and Powers, A.C. (2012). Tamoxifen-Induced Cre-loxP Recombination Is Prolonged in Pancreatic Islets of Adult Mice. *PLoS ONE* 7, e33529.
- Reinert, R.B., Brissova, M., Shostak, A., Pan, F.C., Poffenberger, G., Cai, Q., Hundemer, G.L., Kantz, J., Thompson, C.S., Dai, C., et al. (2013). Vascular endothelial growth factor-a and islet vascularization are necessary in developing, but not adult, pancreatic islets. *Diabetes* 62, 4154–4164.
- Reinert, R.B., Cai, Q., Hong, J.-Y., Plank, J.L., Aamodt, K., Prasad, N., Aramandla, R., Dai, C., Levy, S., Pozzi, A., et al. (2014). Vascular endothelial growth factor coordinates islet innervation via vascular scaffolding. *Development*, in press. Published online March 18, 2014. <http://dx.doi.org/10.1242/dev.098657>.
- Ricardo, S.D.S., van Goor, H.H., and Eddy, A.A.A. (2008). Macrophage diversity in renal injury and repair. *J. Clin. Invest.* 118, 3522–3530.
- Rieck, S., and Kaestner, K.H. (2010). Expansion of beta-cell mass in response to pregnancy. *Trends Endocrinol. Metab.* 21, 151–158.
- Sand, F.W., Hörnblad, A., Johansson, J.K., Lorén, C., Edsbacke, J., Ståhlberg, A., Magenheimer, J., Ilovich, O., Mishani, E., Dor, Y., et al. (2011). Growth-limiting role of endothelial cells in endoderm development. *Dev. Biol.* 352, 267–277.
- Sharpe, E.E., 3rd, Teleron, A.A., Li, B., Price, J., Sands, M.S., Alford, K., and Young, P.P. (2006). The origin and in vivo significance of murine and human culture-expanded endothelial progenitor cells. *Am. J. Pathol.* 168, 1710–1721.
- Sica, A., and Mantovani, A. (2012). Macrophage plasticity and polarization: in vivo veritas. *J. Clin. Invest.* 122, 787–795.
- Soriano, P. (1999). Generalized lacZ expression with the ROSA26 Cre reporter strain. *Nat. Genet.* 21, 70–71.
- Tsunawaki, S., Sporn, M., Ding, A., and Nathan, C. (1988). Deactivation of macrophages by transforming growth factor-beta. *Nature* 334, 260–262.
- Urbán, V.S., Kiss, J., Kovács, J., Gócsa, E., Vas, V., Monostori, E., and Uher, F. (2008). Mesenchymal stem cells cooperate with bone marrow cells in therapy of diabetes. *Stem Cells* 26, 244–253.
- Vasir, B., Jonas, J.C., Steil, G.M., Hollister-Lock, J., Hasenkamp, W., Sharma, A., Bonner-Weir, S., and Weir, G.C. (2001). Gene expression of VEGF and its receptors Flk-1/KDR and Flt-1 in cultured and transplanted rat islets. *Transplantation* 71, 924–935.
- Wang, Y.V., Leblanc, M., Fox, N., Mao, J.-H., Tinkum, K.L., Krummel, K., Engle, D., Piwnicka-Worms, D., Piwnicka-Worms, H., Balmain, A., et al. (2011). Fine-tuning p53 activity through C-terminal modification significantly contributes to HSC homeostasis and mouse radiosensitivity. *Genes Dev.* 25, 1426–1438.
- Ward, T.H., Cummings, J., Dean, E., Greystoke, A., Hou, J.M., Backen, A., Ranson, M., and Dive, C. (2008). Biomarkers of apoptosis. *Br. J. Cancer* 99, 841–846.
- Yoshitomi, H., and Zaret, K.S. (2004). Endothelial cell interactions initiate dorsal pancreas development by selectively inducing the transcription factor Ptf1a. *Development* 131, 807–817.
- Zhang, H., Fujitani, Y., Wright, C.V.E., and Gannon, M. (2005). Efficient recombination in pancreatic islets by a tamoxifen-inducible Cre-recombinase. *Genesis* 42, 210–217.